Polymer 49 (2008) 4259–4270

Contents lists available at ScienceDirect

Polymer

journal homepage: www.elsevier.com/locate/polymer

Ductile–brittle transition controlled by isothermal crystallization of isotactic polypropylene and its blend with poly(ethylene-*co*-octene)

Yongyan Pang [a,c], Xia Dong [a,*], Kaipeng Liu [b], Charles C. Han [a], Erqiang Chen [b], Dujin Wang [a,*]

[a] Beijing National Laboratory for Molecular Sciences, Key Laboratory of Engineering Plastics, State Key Laboratory of Polymer Physics and Chemistry, Institute of Chemistry, Chinese Academy of Sciences, Beijing 100190, China
[b] Beijing National Laboratory for Molecular Sciences, Department of Polymer Science and Engineering and the Key Laboratory of Polymer Chemistry and Physics of Ministry of Education, College of Chemistry and Molecular Engineering, Peking University, Beijing 100871, China
[c] Graduate School of Chinese Academy of Sciences, Beijing 100190, China

ARTICLE INFO

Article history:
Received 21 April 2008
Received in revised form 11 July 2008
Accepted 11 July 2008
Available online 18 July 2008

Keywords:
Ductile–brittle transition
Isothermal crystallization
Isotactic polypropylene

ABSTRACT

The correlation between crystalline morphology development and tensile properties of isotactic polypropylene (iPP) and its blend with poly(ethylene-*co*-octene) (PEOc) was investigated to study the ductile–brittle transition (DBT) in fracture modes. The sample processing strategy and the scientific observations have never been reported previously. The samples were first isothermally crystallized at 130 °C, 123 °C or 115 °C for a wide range of crystallization times, and then quenched to 35 °C for characterization. It was found that the crystallization conditions including crystallization temperature and time governed the crystalline morphology and even the tensile properties of iPP and the iPP/PEOc (80/20) blend. The lower the crystallization temperature, the shorter the crystallization time was needed for the occurrence of DBT, and the sharper the transition would be. The addition of the elastomer component delayed the DBT occurrence for the iPP/PEOc blend in terms of the crystallization time, owing to the fact that the existence of PEOc domains between the iPP lamellar stack regions or at the iPP spherulitic boundaries enhanced the ductility of the blend. The X-ray diffraction results displayed the oriented and destroyed crystalline structure characterizing the ductile fracture, while unoriented structure describing the brittle failure. The DBT is closely related to the crystal perfection, and factors such as the crystallization temperature and time and the compositions have been proven to be significant variables in determining the DBT occurrence.

1. Introduction

Due to the promising industrial applications, in recent years, isotactic polypropylene (iPP) and poly(ethylene-*co*-octene) (PEOc) blends have been extensively investigated from various aspects, including morphology evolution, rheological properties, crystallization and melting behaviors, mechanical properties, etc. [1–11]. There have been a great many reports focusing on the mechanical properties, especially for impact toughness and tensile properties of the blends [1,3–7]. The impact toughness of the iPP/PEOc blends is greatly enhanced compared with that of pure iPP, attributed to the fact that the elastomeric component stimulates the yielding or crazing of iPP matrix, thus dissipating the impact energy. The yield strength and Young's modulus of the blend are depressed, while the elongation at break and break strength are increased within a limited elastomer concentration range, promoting the ductility and even the strain hardening.

For the investigation of thermoplastics including polyolefin elastomers, the concept of "ductile–brittle transition" (DBT) [6,12–21] is generally employed to describe the deformation style and consequently used to estimate the mechanical properties of polymeric materials from industrial points of view. In impact test, the term is always used to dictate a sudden impact toughness change from ductile failure to brittle failure, where a critical interparticle distance can be obtained [12–14, 21]. In tensile test, the DBT is also commonly understood due to the deformation manner alteration from shear yielding to crazing. The previous studies [15–17] tended to interpret the transition in terms of the competition between shear banding initiation stress and the crazing initiation stress. In specific, crazing dominates the deformation manner when shear banding initiation stress exceeds the crazing initiation stress, and conversely, shear yielding failure will be dominant. The transition takes place as the two kinds of initiation stress are nearly equivalent with each other. Generally, the brittle deformation occurs when the sample breaks at its maximum load or the sample manifests a load drop after the yield point with little or no necking [15]. According to Mandelkern et al. [18–20], the ductile fracture is defined when the draw ratio at break is greater

* Corresponding authors. Tel.: +86 10 82618533; fax: +86 10 62521519.
E-mail addresses: xiadong@iccas.ac.cn (X. Dong), djwang@iccas.ac.cn (D. Wang).

0032-3861/$ – see front matter © 2008 Elsevier Ltd. All rights reserved.
doi:10.1016/j.polymer.2008.07.017

than unity, while the brittle deformation takes place when the draw ratio is about 1. They systematically investigated the influencing factors on DBT in tensile deformation of crystalline polymers, from the respects of molecular parameters to crystallinity degree, and so on. Yang et al. studied the DBT of iPP/PEOc blends via changing the tensile speeds and found that the specimens were generally tensile fractured in a ductile manner exerted with lower crosshead speeds, and in a brittle fracture applied with higher crosshead speeds [6]. It was found that the higher content of rubber phase, higher testing temperature and slower testing speeds are all favorable factors for ductile deformation [6,15,17].

The influence of molecular parameters, compositions and testing conditions on DBT has been extensively investigated [6,15,17,19,22], however, the morphology evolution and crystallization controlled by special strategy have seldom been considered [18,20]. In a previous report, the gradual destruction of ductility of iPP and the iPP/PEOc blend was observed due to the progressive crystal perfection via decreasing the cooling rate under non-isothermal crystallization [11]. The main objective of the present work is to elucidate DBT in tensile deformation via isothermal crystallization strategy, i.e., changing isothermal crystallization temperature and time. Although Mandelkern et al. [18,20] have ever investigated the dependence of DBT on the crystallinity, however, the crystallization time has not been considered as an important factor, which will be proven of great significance in this work. Furthermore, the tensile properties of the iPP/PEOc blend were compared with those of pure iPP to essentially elucidate the effect of the addition of elastomer component on the occurrence of DBT.

2. Experimental

2.1. Materials and blending

Isotactic polypropylene (iPP 1300) with $M_w = 4.1 \times 10^5$ and $M_w/M_n \sim 4$ was supplied by Beijing Yanshan Petrochemical Co., Ltd. Poly(ethylene-*co*-octene) (PEOc, Engage 8150) with $M_w = 1.5 \times 10^5$, $M_w/M_n \sim 2$, and 30.6 wt.% of 1-octene comonomer was purchased from DuPont–Dow elastomers. The molecular weight and its distribution were gained from gel permeation chromatography. The comonomer content was calculated based on ^{13}C NMR spectra.

The iPP/PEOc (80/20) blend containing 20 wt.% of PEOc was prepared using a co-rotating twin screw extruder (TSE-30A) with an aspect ratio of $L/D = 40$. The temperatures from feed to die zones were 180 °C, 190 °C, 200 °C, 220 °C, 220 °C, 220 °C, 220 °C, 200 °C, 190 °C and 180 °C, respectively. The screw speed was set at 150 rpm. The blending was performed twice to ensure uniformly dispersed morphology. For comparison, pure iPP underwent the same treatment as the blend.

2.2. Optical microscopic observation

The crystalline morphology of iPP and the iPP/PEOc (80/20) blend was observed using a BX51 Olympus polarized optical microscope (POM) connected with a Linkam THMS600 hot stage under nitrogen atmosphere. The polymer films for POM observation were ca. 30 μm in thickness prepared with a homemade hot press. The films were first melted at 200 °C and then cooled to 130 °C, 123 °C or 115 °C, respectively, for isothermal crystallization with a set of times at a cooling rate of 100 °C/min with the aid of liquid nitrogen. After the isothermal crystallization process, the samples were quenched to 35 °C at a rate of 100 °C/min. The procedures are identical with the sample preparation processes for tensile tests, which will be described below. The polarized optical micrographs were taken during the isothermal crystallization process or after the samples were quenched to 35 °C.

2.3. Crystallization characterization

The melting and crystallization behaviors of samples prepared via isothermal crystallization were studied with a Perkin–Elmer differential scanning calorimeter (model DSC7) at a heating rate of 5 °C/min under nitrogen protection. The samples used were taken from the remains of the iPP or the iPP/PEOc (80/20) blend sheets after the tensile bars were cut out. Melting temperatures and fusion enthalpy were obtained from the heating scans to estimate the crystal perfection. The instrument was calibrated with standard Indium.

2.4. Tensile test

2.4.1. Sample preparation

The samples for tensile tests were prepared via isothermal crystallization processes, which were described as follows.

The pellets of iPP or the iPP/PEOc (80/20) blend were preheated at 200 °C in an LP-S-50 compression molder for 5 min (t_h), pressed for 2 min (t_p) with the pressure of 5 MPa, and then quickly transferred to a TDM-50-2 compression molder with the pressure set at 5 MPa and temperature set at 130 °C, 123 °C, or 115 °C, respectively, for isothermal crystallization. All the samples were isothermally crystallized for a wide range of time periods, i.e., 2 min, 5 min, 10 min, 20 min, 30 min, 60 min. After the isothermal crystallization procedure, the samples were quickly transferred to another TDM-50-2 compression molder with the temperature set at 35 °C and pressure at 5 MPa for 5 min to cool down. The schematic illustration of the primary sheet preparation process is shown in Fig. 1.

2.4.2. Extensional deformation test

According to GB13022-91, the tensile dumbbell-shaped bars were cut out from the primary sheets using an RP/PCP pneumatic serving machine with the rectangular dimensions of length 25 mm, width 6 mm, and thickness 1 mm. The bars were held in an LRH-250A constant temperature and humidity cultivation cabinet for 48 h to keep temperature (23 °C) and humidity (50%) constant before testing. The tensile tests were performed with an Instron 3365 Universal mechanical testing machine at room temperature at a crosshead speed of 50 mm/min. The extension was imposed until the tensile bars were fractured. The results of tensile properties presented were the average of five samples.

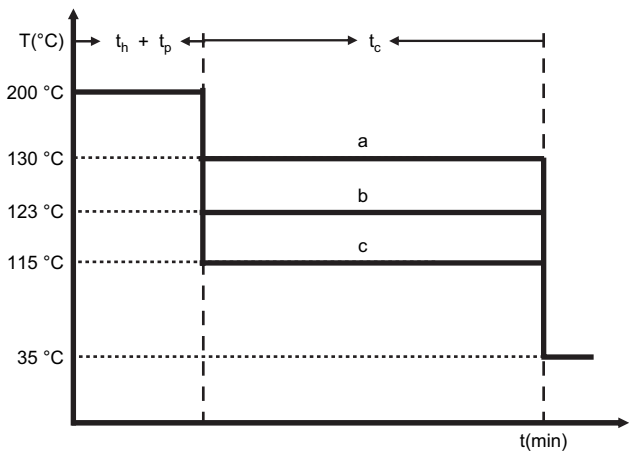

Fig. 1. Schematic illustration of sample preparation processes. The samples were first preheated at 200 °C for 5 min (t_h) and then kept under 5 MPa for 2 min (t_p), followed by an isothermal crystallization at 130 °C (a), 123 °C (b), 115 °C (c), respectively, for various times (t_c) and finally quenched to 35 °C.

2.5. Small angle X-ray scattering

Small angle X-ray scattering (SAXS) measurement of undeformed specimens was performed with an Anton Paar SAXSees system using Cu Kα radiation ($\lambda = 1.54$ Å) at room temperature. The samples were undeformed regions taken from the remains of the iPP or the iPP/PEOc blend sheets after the tensile bars were cut out. The X-ray exposure time was 3 min.

2.6. Wide angle X-ray diffraction

The two-dimensional wide angle X-ray diffraction (2D WAXD) characterization was performed using a Bruker D8 Discover diffractometer equipped with GADDS as a 2D detector in transmission mode. The X-ray source (Cu Kα, $\lambda = 1.54$ Å) was provided by 3 kW ceramic tubes, and the diffraction peak positions were calibrated with silicon powder ($2\theta > 15°$) and silver behenate ($2\theta < 10°$). The diffraction patterns for deformed regions of fractured specimens were investigated at room temperature with X-ray exposure time of 5 min. The point-focused X-ray beam was aligned perpendicular to the stretching direction. The background scattering was recorded and subtracted from the sample patterns.

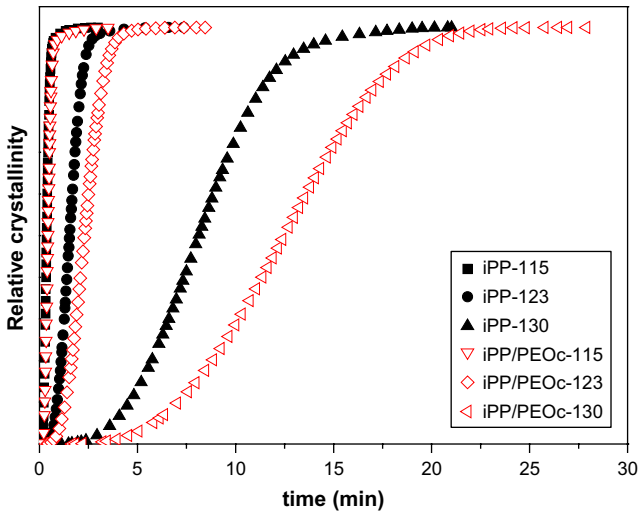

Fig. 2. Crystallinity variation of iPP and the iPP/PEOc (80/20) blend undergoing isothermal crystallization at 130 °C, 123 °C, and 115 °C, respectively.

3. Results and discussion

3.1. Morphology investigation

3.1.1. Pure iPP

The isothermal crystallization of iPP and the iPP/PEOc (80/20) blend at 130 °C, 123 °C, or 115 °C was investigated at first. The integrated curves of crystallinity degree in the course of isothermal crystallization are displayed in Fig. 2, which indicates that the crystallization rate increases as the crystallization temperature decreases for both iPP and the iPP/PEOc blend and that it is depressed by the addition of PEOc component. Therefore, it sounds an interesting route to control the crystallization morphology and subsequent mechanical properties by restricting the isothermal crystallization to different levels of iPP and the iPP/PEOc blend.

Fig. 3a and b shows that if iPP was isothermally crystallized at 130 °C for 2 min, 5 min or 10 min, only a few spherulites were formed, and when the samples were quenched to 35 °C, small crystallites quickly grown from uncrystallized melt and impinged on each other, resulting in a morphology of large spherulites surrounded by a great many small crystallites. For the specimen undergoing isothermal crystallization for 20 min and subsequent quenching, the morphology formed was large spherulites with a few small crystallites locating at the iPP spherulitic boundaries. When the iPP samples were further crystallized for 30 min and

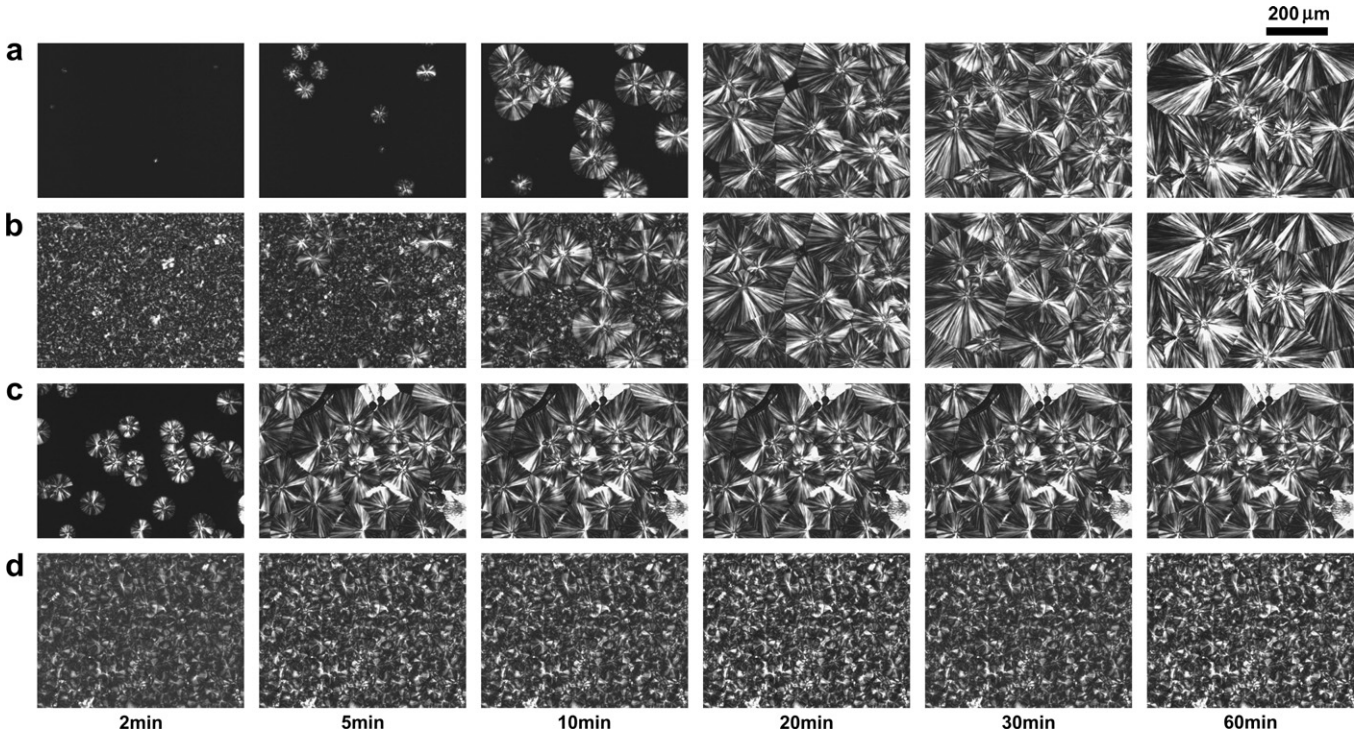

Fig. 3. POM images of iPP isothermally crystallized at 130 °C for various times (a) and then quenched to 35 °C (b). In situ crystalline morphology development of iPP isothermally crystallized at 123 °C (c) and at 115 °C (d) for various times.

60 min, the primary crystallization was nearly accomplished by forming large spherulites with sharp boundaries. Even though the samples were quenched to 35 °C, the final morphology showed no obvious change.

The in situ isothermal crystallization of iPP at 123 °C (Fig. 3c) shows faster crystallization rate than that at 130 °C, consistent with the result in Fig. 2. When iPP was isothermally crystallized for 2 min, most of the spherulites were isolated and have small size. When crystallized for 5 min, most of the iPP spherulites impinged on each other. Given longer time, the primary crystallization was nearly accomplished with large spherulites. The results clearly demonstrate that a great many small crystallites could come into being during the quenching after the isothermal crystallization for 2 min, and only a few were observed after crystallization for 5 min, while the subsequent quenching had no visible influence on the crystallization morphology of other samples (not shown here). When iPP was isothermally crystallized at 115 °C, the crystallization was much faster. The in situ morphology development in Fig. 3d shows that the primary crystallization has been accomplished almost within 2 min, and the morphology displays nearly no visible change during further annealing. The crystalline morphology after subsequent quenching is almost the same as that formed during isothermal crystallization, i.e., small crystallites with low perfection. Maybe long-term annealing has some kind of effect on the lamellar thickening and crystal perfection [23–25], however, it is difficult to be resolved by the optical microscope and will be discussed later.

3.1.2. iPP/PEOc blend

The morphology development for the iPP/PEOc (80/20) blend (Fig. 4) isothermally crystallized at 130 °C, 123 °C and 115 °C for various times is similar to that of pure iPP (Fig. 3) except for the defective iPP crystals in the blend. The crystalline difference between pure iPP and the iPP/PEOc blend is due to the existence of PEOc component. The dark points in the POM images are believed to be the trapped PEOc inclusions in iPP matrix [8,10,11].

3.2. DSC characterization on crystallization behavior

When iPP was isothermally crystallized at 130 °C for 2 min, 5 min, 10 min, and then quenched to 35 °C, dual melting peaks emerged (Fig. 5a_1), which may be assigned to lamellae of different thicknesses, consistent with previous studies [23,26]. As the sample was isothermally crystallized for 20 min, the lower melting peak is largely depressed, indicating the decrease of the content of the crystals with thinner lamellae. Further increasing the crystallization to 30 min and 60 min, only a single sharp melting peak was detected. Decreasing the isothermal crystallization temperature (Fig. 5a_2 and a_3), it was found that the dual melting peaks only appeared at very early crystallization stage, i.e., 2 min and 5 min for 123 °C, only 2 min for 115 °C. For all the other time periods, only a single melting peak was found. These dual melting peaks during the heating process of iPP specimens might be due to the melting–recrystallization from more defective crystals [25,27,28]. The melting parameters of pure iPP are summarized in Table 1. The crystallinity of iPP was roughly calculated based on the melting enthalpy according to previous investigations [11].

The iPP/PEOc (80/20) blend showed similar crystallization behavior as pure iPP at the given isothermal crystallization conditions. Dual or broad melting peaks were observed for the iPP/PEOc blend isothermally crystallized at 130 °C for 2 min, 5 min, 10 min, 20 min and 30 min, and a single peak for 60 min (Fig. 5b_1). Similarly, dual melting peaks emerged for samples crystallized at 123 °C for 2 min, 5 min and 10 min (Fig. 5b_2), and at 115 °C for 2 min and 5 min (Fig. 5b_3). The melting parameters of the iPP/PEOc blend are summarized in Table 2. The normalized crystallinity degree of iPP component and the total crystallinity were calculated according to previous report [11].

By comparing the melting behaviors of pure iPP and the iPP/PEOc blend, some concluding remarks can be drawn. First, the crystallization rate of iPP in the blend is depressed compared with that of pure iPP, as the addition of elastomer may hinder the iPP crystals from getting higher perfection. This finding is in good

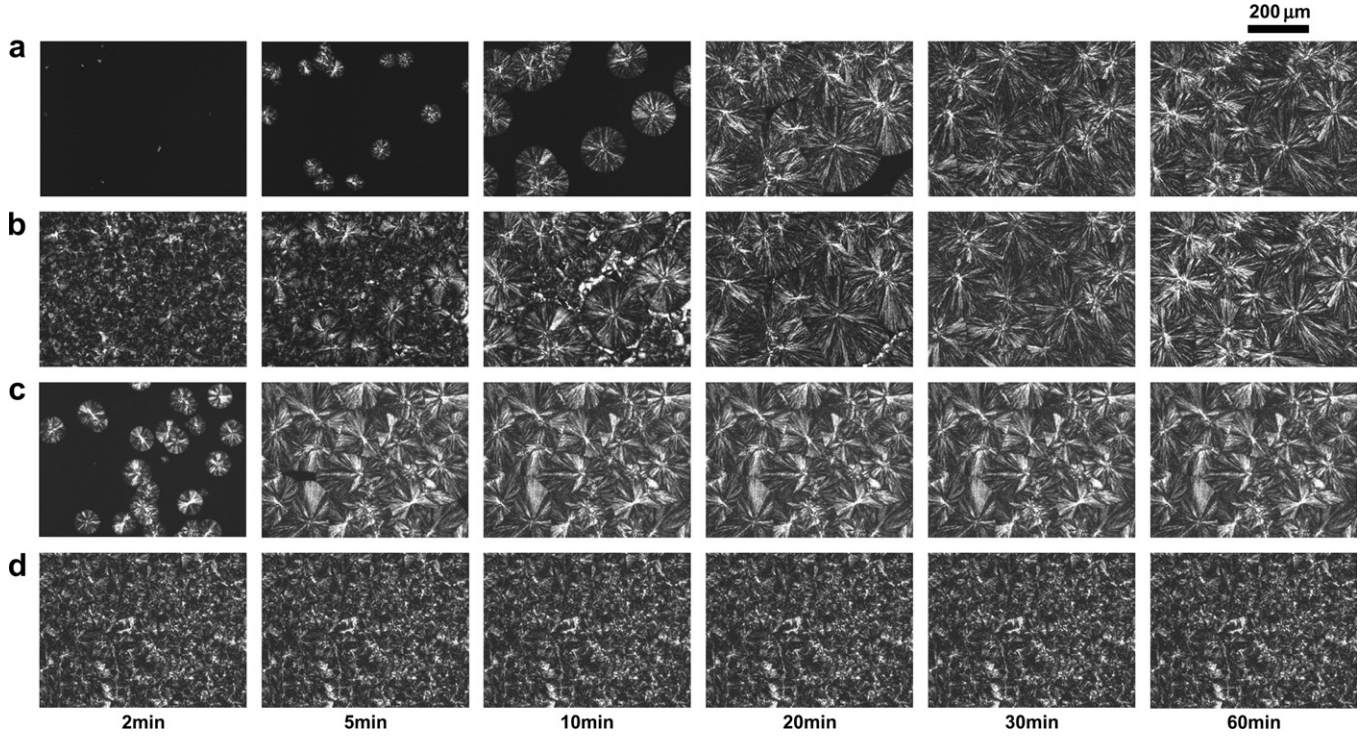

Fig. 4. POM images of the iPP/PEOc (80/20) blend isothermally crystallized at 130 °C for various times (a) and then quenched to 35 °C (b). In situ crystalline morphology development of the iPP/PEOc (80/20) blend isothermally crystallized at 123 °C (c) and at 115 °C (d) for various times.

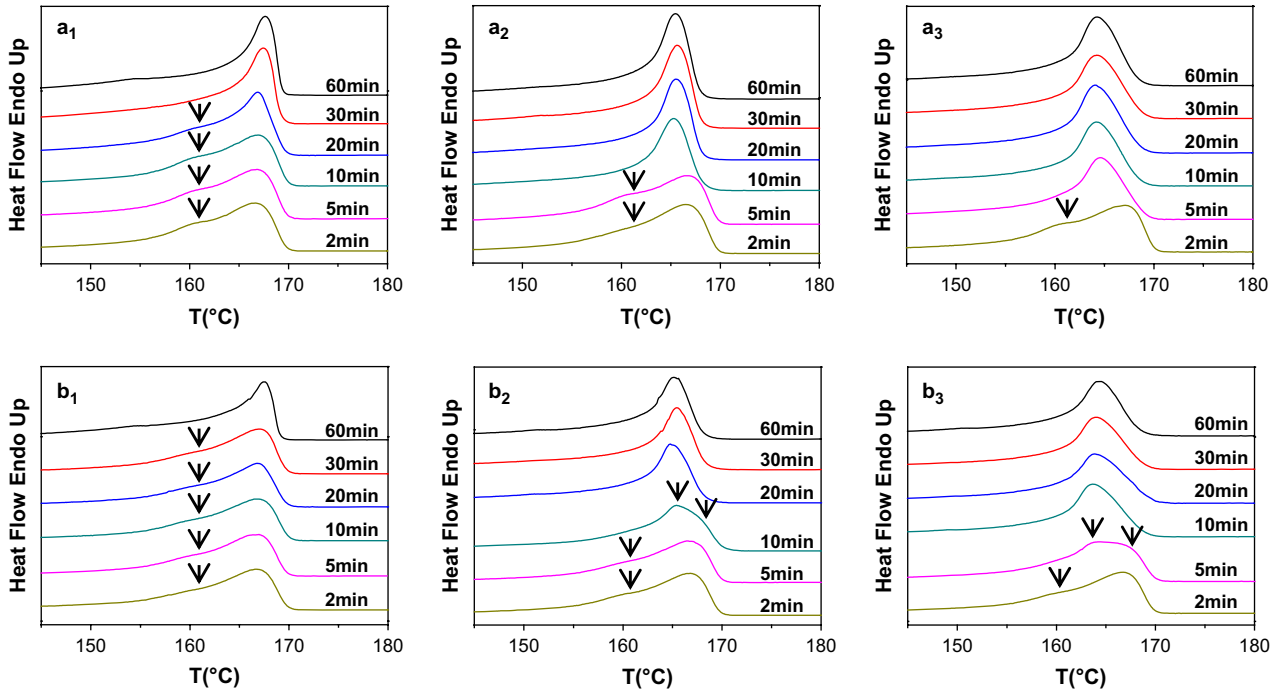

Fig. 5. DSC heating scans (5 °C/min) for iPP (a) and the iPP/PEOc (80/20) blend (b) specimens prepared via isothermal crystallization at 130 °C (1), 123 °C (2), 115 °C (3), respectively, for various times and then quenched to 35 °C.

Table 1
Melting parameters related to iPP isothermally crystallized at 130 °C, 123 °C and 115 °C, respectively, for various times

T (°C)	Parameter	Crystallization time(min)					
		2	5	10	20	30	60
130	Onset (°C)	157.8	158.0	158.8	162.0	163.6	164.0
	T_{m1} (°C)	160.8	160.9	160.9	160.5		
	T_{m2} (°C)	166.6	166.8	166.9	166.9	167.5	167.6
	X_c^{iPP} (%)	41.6	43.1	44.2	46.3	49.8	50.5
123	Onset (°C)	156.8	156.9	161.4	162.3	162.1	162.0
	T_{m1} (°C)	160.7	160.9				
	T_{m2} (°C)	166.5	166.5	165.3	165.5	165.6	165.5
	X_c^{iPP} (%)	41.6	43.2	45.3	48.4	50.5	50.8
115	Onset (°C)	156.2	160.4	160.4	160.5	160.4	160.7
	T_{m1} (°C)	160.8					
	T_{m2} (°C)	166.7	164.6	164.2	164.1	164.2	164.2
	X_c^{iPP} (%)	42.4	43.8	46.9	46.6	45.4	47.0

Table 2
Melting parameters related to the iPP/PEOc (80/20) blend isothermally crystallized at 130 °C, 123 °C and 115 °C for various times

T (°C)	Parameter	Crystallization time (min)					
		2	5	10	20	30	60
130	Onset (°C)	158.6	157.8	157.1	158.9	157.9	163.9
	T_{m1} (°C)	160.7	160.4	160.4	160.4	160.5	
	T_{m2} (°C)	166.6	167.0	166.7	166.8	167.0	167.5
	X_c^{iPP} (%)	43.2	43.6	44.7	45.4	46.3	50.4
	X_c^t (%)	36.3	36.5	37.5	38.4	39.3	42.7
123	Onset (°C)	158.2	157.1	160.3	161.7	162.3	162.2
	T_{m1} (°C)	160.5	160.5	165.1			
	T_{m2} (°C)	166.8	166.5	166.8	164.8	165.4	165.1
	X_c^{iPP} (%)	43.9	44.0	46.1	48.1	49.2	48.9
	X_c^t (%)	36.9	37.5	39.1	40.0	41.6	40.7
115	Onset (°C)	157.2	158.9	159.9	160.3	160.2	160.4
	T_{m1} (°C)	160.4	164.3				
	T_{m2} (°C)	166.7	167.0	163.7	163.9	164.0	164.4
	X_c^{iPP} (%)	43.4	46.7	47.5	47.7	47.9	47.6
	X_c^t (%)	36.9	39.4	40.4	40.6	40.7	39.6

accordance with Fig. 2, which also displays the faster crystallization rate for iPP. Second, the crystallinity levels of both pure iPP and the iPP component in the blend roughly increase with the prolongation of isothermal crystallization at the three temperatures, indicating the gradual weakening of interspherulitic and interlamellar connections according to previous report [11]. Third, compared with the crystallinity of pure iPP, the total crystallinity of the iPP/PEOc (80/20) blend is decreased with the addition of elastomer component (Tables 1 and 2).

3.3. Ductile–brittle transition

In order to show the effect of crystal perfection in the progress of isothermal crystallization on the fracture mode alteration, the stress–strain curves of iPP and the iPP/PEOc (80/20) blend isothermally crystallized at 130 °C were selected as examples. It is illustrated in Fig. 6a that when iPP was first crystallized at 130 °C for 2 min, 5 min, and 10 min, then quenched to 35 °C, the corresponding tensile bars were fractured in a ductile manner in strain hardening zone, possessing larger elongation at break and larger break strength. When crystallized at 130 °C for 20 min, the failure of iPP bars took place in the necking zone, manifesting the lowest break strength. As for iPP crystallized for 30 min and 60 min, the samples were failed in a brittle fracture mode in strain softening zone, showing shorter elongation at break and larger break strength. So, it is deduced that the ductile–brittle transition for iPP crystallized at 130 °C took place between 10 min and 30 min. It is shown in Fig. 6b that when the iPP/PEOc (80/20) blend was isothermally crystallized at 130 °C for 2 min, 5 min, 10 min, 20 min and 30 min, respectively, the samples were fractured in ductile deformation in strain hardening zone, while crystallized for 60 min, the specimen was fractured in strain softening zone with the elongation at break at about 40%, displaying the fracture in a brittle manner according to the previous reports [18–20]. Consequently, the DBT occurs between 30 min and 60 min when the blend was crystallized at 130 °C, implying that compared with pure iPP, the ductile–brittle transition of the iPP/PEOc (80/20)

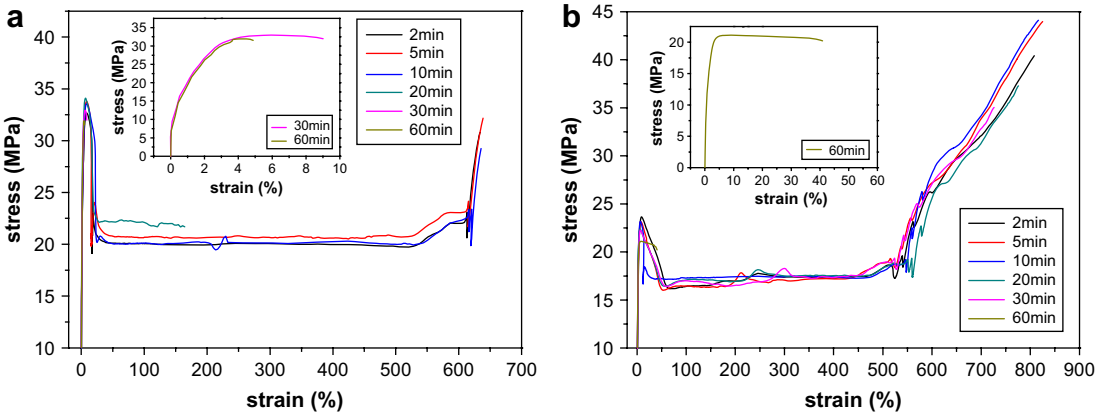

Fig. 6. Stress–strain curves of pure iPP (a) and the iPP/PEOc (80/20) blend (b) specimens undergoing different isothermal crystallization times at 130 °C.

blend is delayed due to the introduction of PEOc component in the blend.

The yield strength, break strength as well as elongation at break of iPP and the iPP/PEOc (80/20) blend will be described in details as follows. With the increase of isothermal crystallization time, the yield strength of iPP crystallized at 130 °C nearly levels off within the observation time scale (Fig. 7a$_1$). The elongation at break shows an almost constant larger value at the first 10 min (strain hardening zone), then a sudden decrease at 20 min (necking zone), at last a constant lower value at 30 min and 60 min (strain softening zone). Correspondingly, the break strength first levels off, then manifests a lowest value, and finally increases to a limited value, i.e., a little bit lower than the yield strength. Therefore, the DBT occurs between the 10 min and 30 min, just as shown in the stress–strain curves (Fig. 6a). As for the iPP samples crystallized at 123 °C (Fig. 7a$_2$), the elongation at break shows higher values (strain hardening zone) at 2 min and 5 min, and suddenly decreases and maintains nearly constant lower values of about 10% (strain softening zone) from 10 min to 60 min, therefore, the DBT occurs between 5 min and 10 min. When crystallized at 115 °C (Fig. 7a$_3$), the iPP specimen was fractured in a ductile manner only for a crystallization time of 2 min, with embrittlement occurring for longer annealing, and as a result, the DBT occurs between 2 min and 5 min.

The DBT in the iPP/PEOc (80/20) blend was also investigated to elucidate the effect of elastomer component on the transition (Fig. 7b). Figs. 7b$_1$ and 6b show that, when iPP/PEOc blend was isothermally crystallized at 130 °C for 2 min, 5 min and 10 min, the samples were fractured in a ductile manner in strain hardening zone, manifesting larger elongation at break and larger break strength. As the crystallization was increased to 20 min or 30 min, the strain hardening is depressed to some extent, resulting in gradual decrease of elongation and break strength. When the blend was crystallized for 60 min, the sample was fractured in a brittle manner in strain softening zone with larger break strength and lower elongation. As a result, the DBT for the iPP/PEOc blend crystallized at 130 °C occurs between 30 min and 60 min, close to 60 min. As the crystallization was performed at 123 °C (Fig. 7b$_2$) for 2 min, 5 min and 10 min, the samples were fractured in ductile deformation in strain hardening zone, and the uptrend of the strain hardening is gradually depressed with isothermal crystallization proceeding. When the blend was crystallized for 20 min, 30 min and 60 min, the samples were fractured in necking zone with almost constant values of elongation and break strength. In the

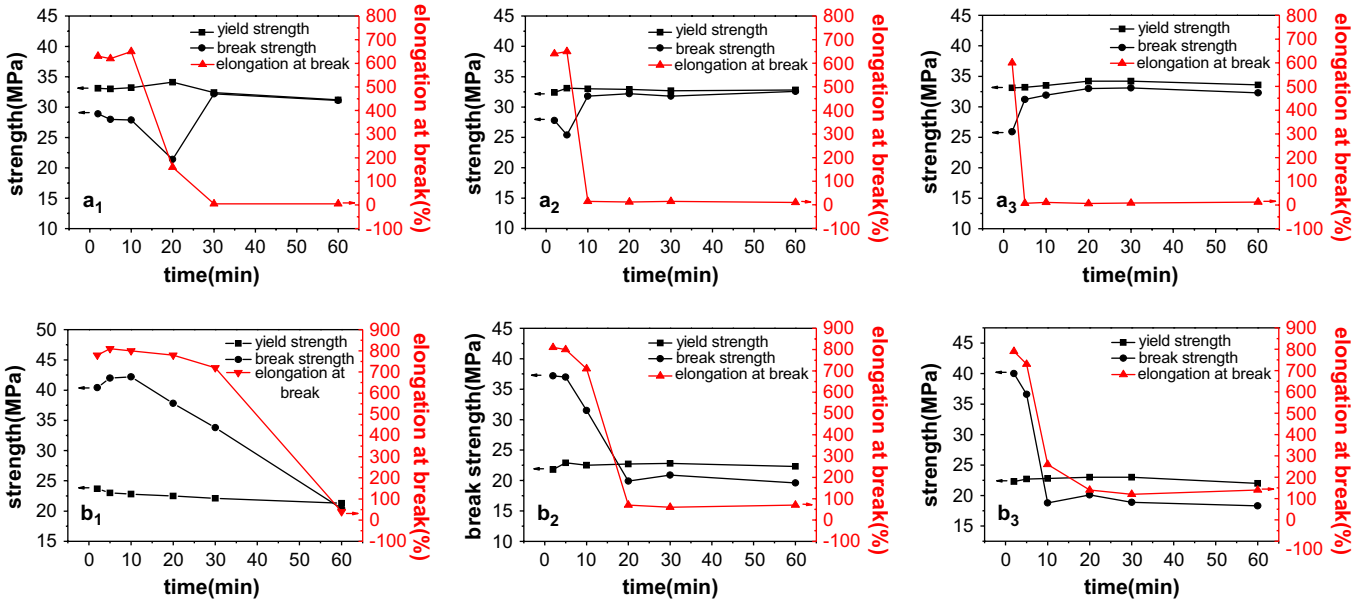

Fig. 7. Tensile properties of iPP (a) and the iPP/PEOc (80/20) blend (b) specimens prepared via isothermal crystallization at 130 °C (1), 123 °C (2), and 115 °C (3), respectively, for various times, and then quenched to 35 °C.

time range, even though the failure occurred in necking zone, the elongation is about 70%, thus, the failure can be taken as brittle deformation [18–20]. As a result, the transition of the deformation modes takes place between 10 min and 20 min. As for the iPP/PEOc blend crystallized at 115 °C (Fig. 7b$_3$), the failure took place in a ductile manner with isothermal crystallization prior to 5 min, and in necking zone with the increase of annealing, exhibiting the elongation at break of ca. 140%. Maybe, the fracture could not be taken as brittle deformation, and the DBT was considered to occur after 5 min. In summary, the time range of DBT under the experimental conditions for iPP and the blend specimens is summarized in Table 3.

In order to clearly show the variation of mechanical properties of iPP and the iPP/PEOc blend, the elongation at break and break strength are plotted in Fig. 8a and b, respectively. It is obvious that for either pure iPP or the iPP/PEOc blend, the lower the crystallization temperature is, the shorter the crystallization time is needed for the DBT to occur, and the sharper the transition will be. However, the elongation at break in brittle failure is about 10% for all pure iPP specimens, while it increases from about 40% (130 °C) to 70% (123 °C) and to 140% (115 °C) for the blend. These indicate that, on one hand, the brittleness for the blend is lower than that of pure iPP, and on the other hand, it decreases with the decrease of the isothermal crystallization temperature. These results imply that the samples comprised of spherulites of lower perfection and smaller sizes are less probably to be fractured in a brittle manner, consistent with the documented results [7,11]. Furthermore, the addition of the elastomer component delays the occurrence of the DBT. That may be the reason why PEOc deserves so much high expectation as the iPP impact modifier. The break strength for both iPP and the iPP/PEOc blend reaches a constant value (obtained in brittle deformation) earlier in time scale with the decrease of the isothermal temperature (Fig. 8b), consistent with the variation of elongation at break. However, the difference between the break strength–time curves of iPP and the blend is quite remarkable. One reason is attributed to the significantly differential strain hardening characteristics, which are very weak for pure iPP, while pronounced for the blend under the experimental conditions. Thus, the values of break strength are always lower than those of the corresponding yield strength for pure iPP, whereas, they are higher for the blend fractured in strong strain hardening zone, and behave lower when the failure would occur in weak strain hardening zone, necking zone or strain softening zone. As a result, there is no intersection between yield strength and break strength for pure iPP (Fig. 7a), but there is for the blend (b). It is understandable that when the brittle failure occurs, the value of break strength must be lower than that of the yield strength, and accordingly, embrittlement for the blend must appear beyond the intersection of break strength and yield strength in time scale. The intersection moves to lower time direction with the decrease of isothermal crystallization temperature. Another difference is that, for iPP specimens, it is not easy to obtain the failure in necking zones at the given observation time points, especially for specimens crystallized at lower temperatures, while it is usual for the blend. As a result, unlike that of the blend, the minimum value of break strength of iPP fractured in necking zone is not easy to be captured. These are the reasons for the distinctive profiles of break strength–time curves for iPP and the iPP/PEOc blend (Fig. 8b).

Table 3
The time range of DBT for iPP and iPP/PEOc (80/20) blend specimens isothermally crystallized at 130 °C, 123 °C, and 115 °C, respectively

Samples	130 °C	123 °C	115 °C
iPP (min)	10–30	5–10	2–5
iPP/PEOc (80/20) (min)	→60	10–20	>5

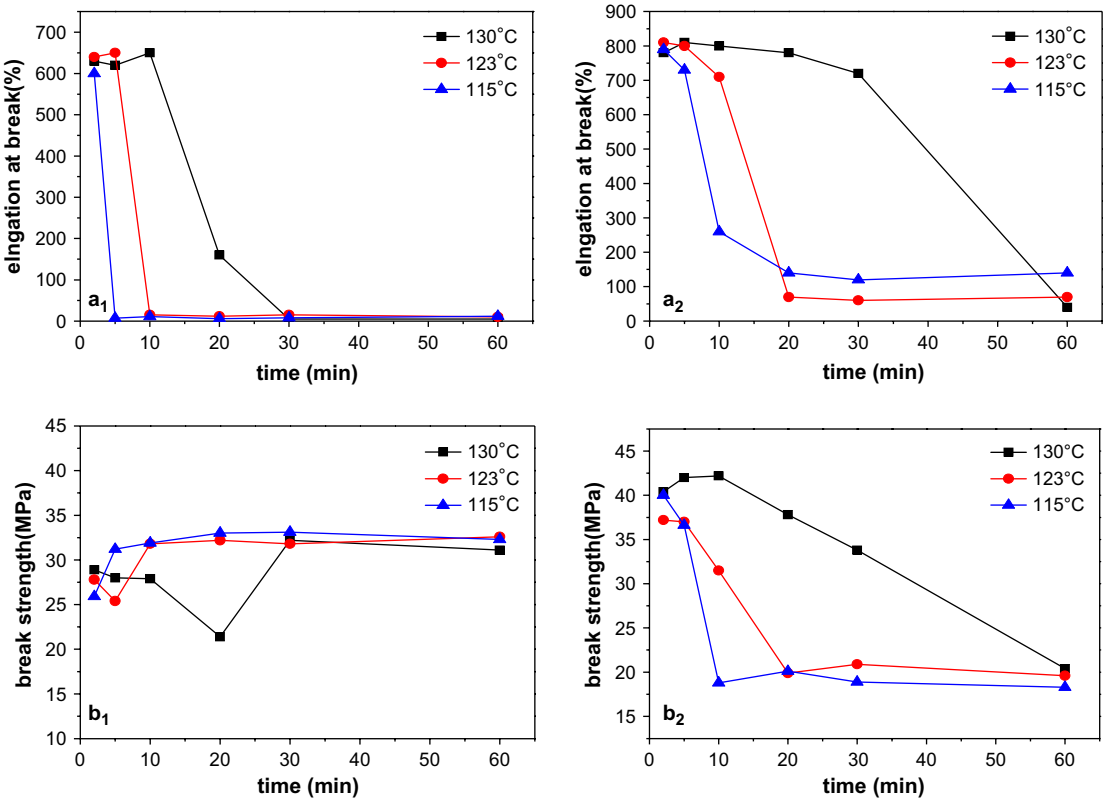

Fig. 8. The elongation at break (a) and break strength (b) for iPP (1) and the iPP/PEOc (80/20) blend (2) isothermally crystallized at 130 °C, 123 °C, and 115 °C, respectively, for different times.

3.4. SAXS characterization on lamellar structure

In order to inspect the lamellar structures and interpret the occurrence of DBT, SAXS techniques were employed. In the Lorentz-corrected SAXS curves (Fig. 9), the scattering maximum is associated with the lamellar periodicity [29–31]. The scattering peaks are broad, indicating a quite broad size distribution of the long periods. Although two kinds of lamellae may exist for specimens undergoing an incomplete isothermal crystallization and a subsequent quenching, displayed by DSC results, however, SAXS is not able to resolve this binary distribution [23].

The averaged long periods (Fig. 10) for iPP and the iPP/PEOc blend were calculated according to the Bragg Law [23,30,31], and their properties are similar. As shown in Fig. 10, for both iPP and the iPP/PEOc blend, the long period increases during the prolonging of the isothermal crystallization, and finally reaches to an equilibrium value at a certain time, which indicates a probable lamellar thickening process during the isothermal crystallization [23–25]. For specimens crystallized at a lower temperature, it seems that the long period reaches to an equilibrium value more quickly as the crystallization proceeds, however, the value is lower than that at higher temperature. It agrees well with the DBT results: crystallized at a lower temperature, the DBT occurs earlier in terms of crystallization time, however, larger brittleness of specimens crystallized at a higher temperature can be obtained till the accomplishment of the primary crystallization. This suggests that the crystalline structure plays an important role influencing the ductile–brittle transition. When the lamellae grow larger, the interlamellar connection will be weaker, and the brittle deformation occurs, which is consistent with the previous investigations [7,11,18,20].

Furthermore, by comparison, the long period of the iPP/PEOc blend is smaller than that of iPP correspondingly. The possible reason is considered that the PEOc domains lie in between the lamellar stacks or at the interspherulitic boundaries rather than the interlamellar regions, thus the long periods are unable to be increased [11]. Besides, the addition of PEOc may suppress the iPP

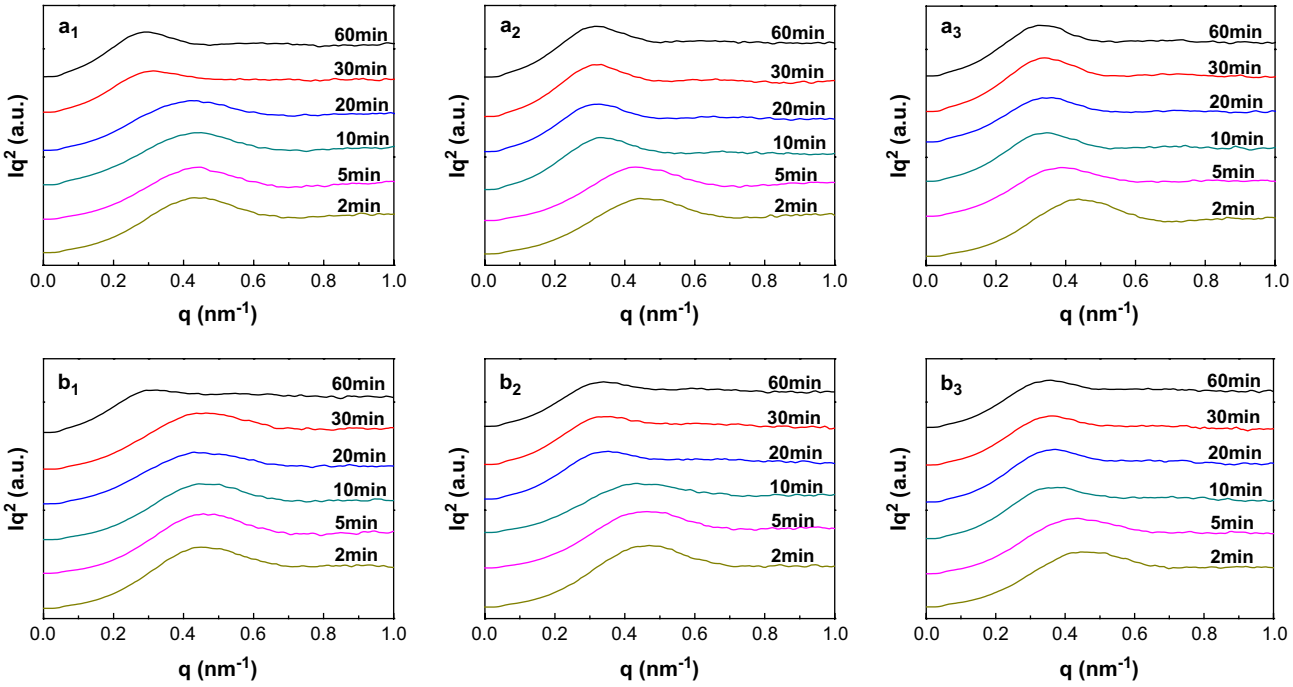

Fig. 9. Lorentz-corrected SAXS profiles of iPP (a) and the iPP/PEOc (80/20) blend (b) specimens isothermally crystallized at 130 °C (1) 123 °C (2) and 115 °C (3), respectively, for various times.

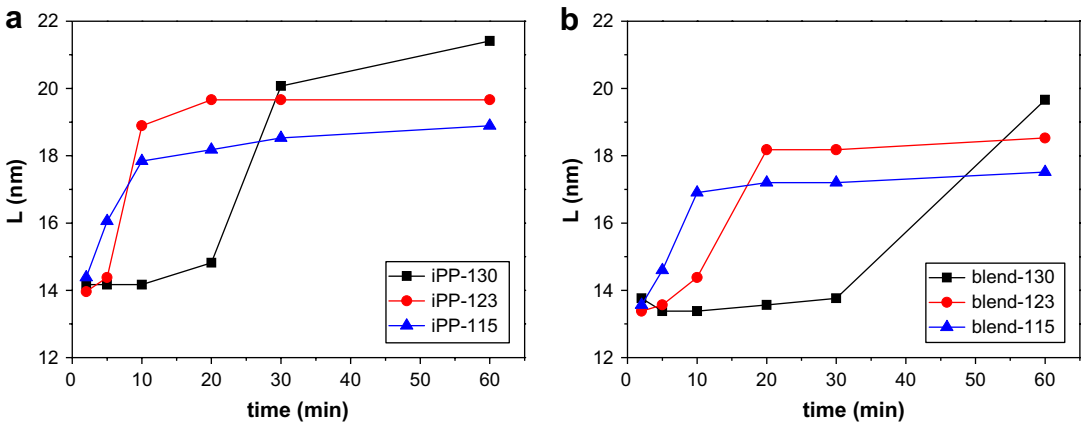

Fig. 10. Variation of long period as a function of isothermal crystallization time for iPP (a) and the iPP/PEOc (80/20) blend (b) at 130 °C, 123 °C and 115 °C, respectively.

crystal perfection in the blend, and therefore may possibly depress its long spacing, which may interpret the delay of the DBT for the blend. Due to the addition of the elastomeric component, the defective lamellar structure of iPP is easily rearranged and deformed under stretching, and the interaction between iPP and PEOc domains promotes more connections and persistence to resist the fracture. Furthermore, the addition of PEOc leads to the lower total crystallinity level and more dull iPP spherulitic boundaries in the blend, and all these result in higher ductility for the blend.

3.5. WAXD characterization on structural deformation

Two-dimensional WAXD characterizations were carried out in order to investigate the structural deformation of iPP (Figs. 11a and 12a). It is displayed in Fig. 11a_1 that iPP specimens exhibit diffraction spots when crystallized at 130 °C for 2 min, 5 min and 10 min, indicating ductile failure involving oriented structure preferentially in the tensile direction. When crystallized for 20 min, the specimen's diffraction pattern changes to arc, indicating the partial orientation for specimens fractured in DBT region. When crystallization time is prolonged to 30 min and 60 min, diffraction rings are observed, suggesting that the specimens fractured in brittle manner maintain nearly unchanged crystalline structure. From the corresponding integrated curves (Fig. 12a_1), it is prominent that the destruction of iPP α-modification after tensile deformation is most obvious for specimens crystallized at 130 °C for 2 min, 5 min and 10 min, then for 20 min, but nearly no destruction for 30 min and 60 min. According to the previous studies [11,32], the broad diffraction peaks are originated from the decrease of crystallite size and disordering of crystalline lattice due to the probable dissociation of original lamellae and molecular shifting under stretching. As for iPP crystallized at 123 °C (Figs. 11a_2 and 12a_2), the fracture mode alteration is between 5 min and 10 min. And for crystallization at 115 °C (Figs. 11a_3 and 12a_3), the transition occurs between 2 min and 5 min.

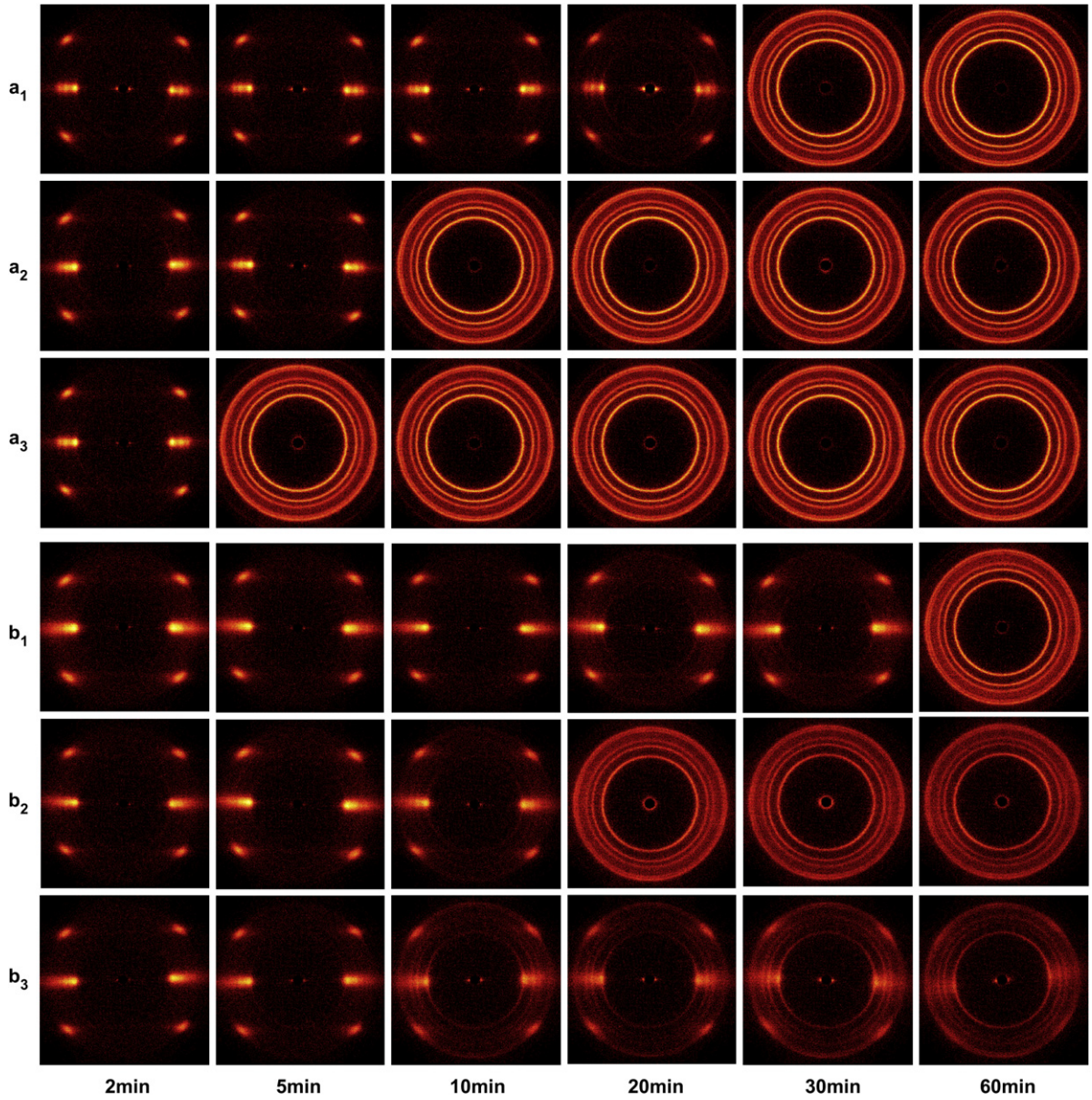

Fig. 11. Two-dimensional WAXD patterns of deformed regions of iPP (a) and the iPP/PEOc (80/20) blend (b) specimens isothermally crystallized at 130 °C (1), 123 °C (2) and 115 °C (3), respectively, for different times. The X-ray incident beam was perpendicular to the stretching direction (the meridian direction).

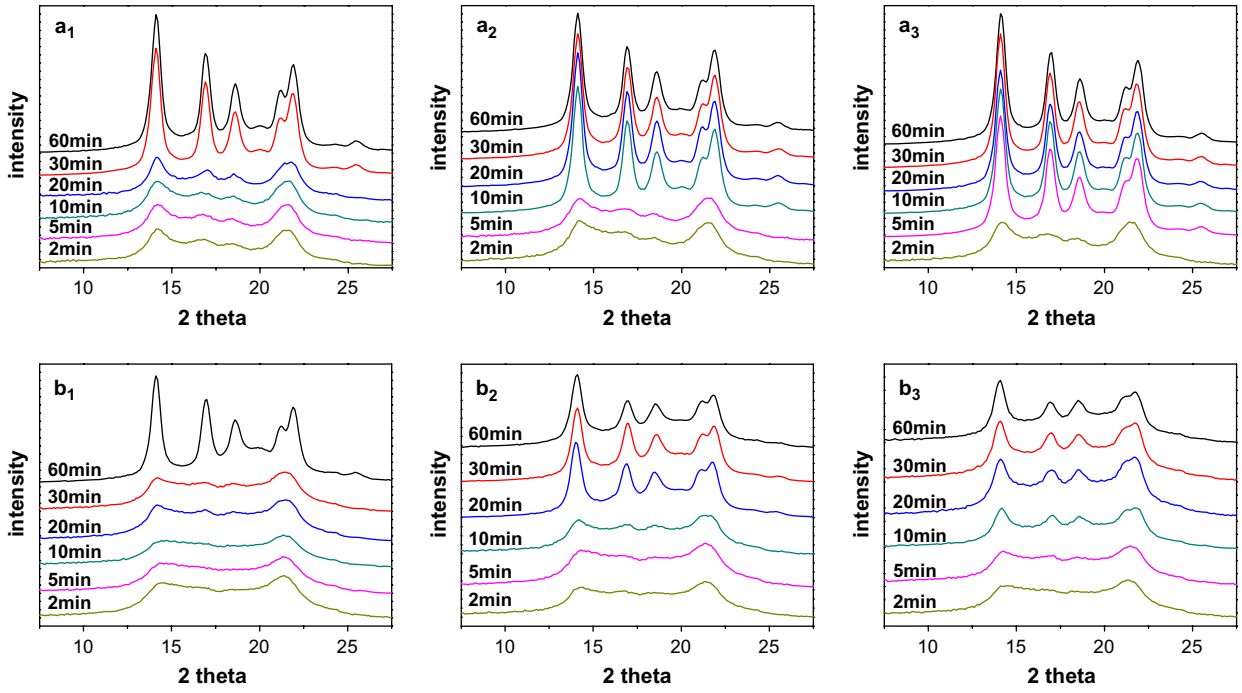

Fig. 12. The corresponding intensity curves of 2D WAXD patterns of deformed regions of iPP (a) and the iPP/PEOc (80/20) blend (b) specimens isothermally crystallized at 130 °C (1), 123 °C (2) and 115 °C (3), respectively, for different times. The X-ray incident beam was perpendicular to the stretching direction (the meridian direction).

The WAXD measurement was also performed for the iPP/PEOc (80/20) blend (Figs. 11b and 12b) for comparison with that of pure iPP. When the blend was isothermally crystallized at 130 °C from 2 min to 30 min, the specimens were fractured in ductile manner with prominent orientation and structural destruction of α modification, which is more obvious for 2 min, 5 min and 10 min than for 20 min and 30 min (Figs. 11b_1 and 12b_1), indicating the gradual destruction of ductility as the increase of crystal perfection. For the specimens crystallized at 123 °C (Figs. 11b_2 and 12b_2), distinctive structural transformation was found between 10 min and 20 min, and weak orientation and structural destruction were observed for deformed specimens with further longer isothermal crystallization. When crystallized at 115 °C (Figs. 11b_3 and 12b_3), the specimens with crystallization time of 2 min and 5 min were fractured in ductile manner, and diffraction arcs were observed from 10 min to 60 min, indicating the partial orientation and structural destruction, consequently, the fractures in such a way cannot be taken as brittle deformation. It is noted that the WAXD profiles for undeformed specimens of iPP and iPP/PEOc blend exhibiting unoriented crystalline structure and sharp integral curves are not shown here.

Based on the above results, it is concluded that the ductile fracture sustains for a longer time period at higher crystallization temperature due to the slower crystallization rate. Moreover, the brittleness is, however, more obvious for the specimens undergoing the accomplishment of primary crystallization at higher temperature. The reasons are considered as follows: on one hand, the spherulites formed with larger sizes are less easily to rearrange themselves under extension, and on the other hand, the interspherulitic connections are weaker, consequently they are more probably fractured in a brittle manner [11].

3.6. Ductile–brittle transition mechanism

It is shown in Fig. 2 and Table 3 that, the ductile deformation occurs for iPP and the iPP/PEOc (80/20) blend specimens are within the accomplishment of the primary crystallization during the isothermal crystallization, and that brittle failures are beyond the primary crystallization. Accordingly, the occurrence of DBT should be more related to the primary crystallization during the isothermal crystallization than the subsequent one during quenching, since the crystals formed in the latter way are of smaller sizes and lower perfection and the boundaries are more diffuse. These are not the favorable factors for the void formation and crack propagation for brittle failure [15–17]. As the isothermal crystallization proceeds, the crystals gradually get higher perfection, and the interlamellar and interspherulitic connections get weaker; these are propitious for brittle failure in crazing mode [11,15–17].

It is speculated that the occurrence of DBT is correlated with the crystallization rate and crystal perfection. As for iPP specimens crystallized at a lower isothermal crystallization temperature, the DBT occurs after a shorter crystallization period, since the crystallization rate is faster and the completion of primary crystallization is earlier, however, the brittleness of specimens is somewhat weaker since crystals formed in this way are of low perfection. As a result, DBT may occur after the accomplishment of the primary crystallization. DBT occurs later at higher crystallization temperature due to the slower crystallization rate, whereas, the brittleness of specimens is much higher due to the enhancement of crystal size and perfection after the completion of the primary crystallization. Consequently, DBT may take place before the accomplishment of the primary crystallization. Based on the above discussion, it is concluded that the crystal perfection and crystallization rate exert inconsistent effect on the occurrence of DBT in time scale.

The origin of the delay of DBT with the addition of elastomer component is speculated on three sides: first, the primary crystallization of iPP component is slowed down in the blend compared with that of pure iPP; secondly, the total crystallinity degree is depressed in the blend, which suppresses the brittleness and therefore enhances the ductility of the blend [11,18,20]; finally, the PEOc domains existing in between lamellar stack regions or at the iPP spherulitic boundaries, which on one hand add to the interconnection between neighboring lamellar stacks and on the other hand, depress the perfection of iPP crystals, and therefore, make iPP lamellae more easily to rearrange themselves under the extensional

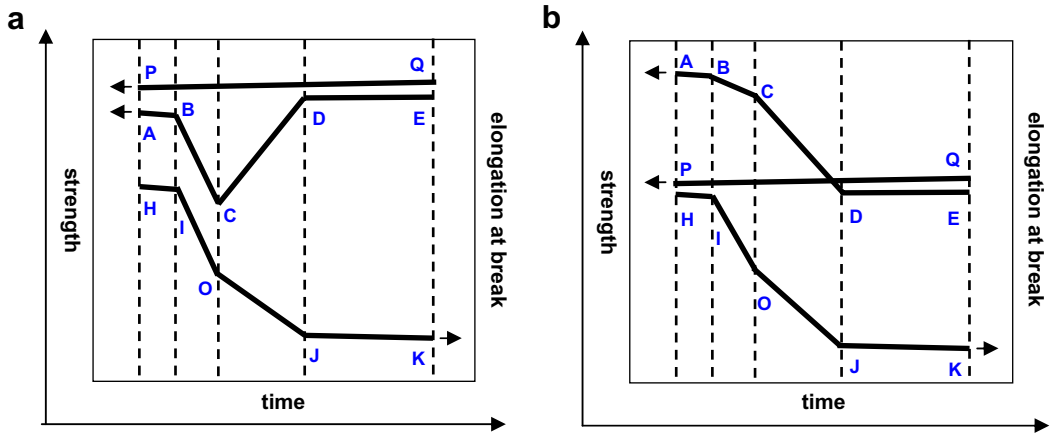

Fig. 13. Schematic illustration of DBT for iPP (a) and the iPP/PEOc (80/20) blend (b) specimens.

deformation [11]. These considerations may also need to be included in the interpretation of the origin of the occurrence of DBT for the blend till the completion of the primary crystallization.

3.7. Schematic of ductile–brittle transition

The schematic illustration (Fig. 13) of DBT is established to show the shifting modes under different isothermal crystallization conditions for iPP and the iPP/PEOc (80/20) blend. The curves P–Q, A–E and H–K stand for yield strength, break strength and elongation at break, respectively. It is noted here that the tensile conditions and the observation time points are fixed as they are. As the isothermal crystallization temperature decreases, the DBT moves to lower time direction, and for much lower temperature, the curves of A–E and H–K observed may be approximately like the horizontal lines as DE and JK. While the temperature increases, the DBT moves to higher time direction, and for much higher temperature, the curves of A–E and H–K observed may also be like the horizontal lines as AB and HI.

The schematic for DBT of iPP is shown in Fig. 13a, and the DBT occurs in the time period of CD (or OJ), and it will change its position with the isothermal crystallization temperature. The fracture in necking zone may not be captured at the fixed observation time points, where the minimum value of break strength yields, therefore, the minimum value may not be able to be obtained. As the isothermal crystallization temperature decreases, the absolute values of slopes of CD and OJ may decrease, and C and O may ascend and descend along *Y* axis, respectively. However, as the temperature increases, the slopes of BC and IO may decrease, and D and J may descend and ascend along *Y* axis, respectively.

Fig. 13b displays the schematic illustration of DBT for the iPP/PEOc blend, and it is noted that J falling on the bottom may be delayed compared with that of D in time scale. As the isothermal crystallization temperature is decreased, C and O may descend along *Y* axis, the slopes of CD and OJ may decrease, the intersection of PQ and CD will move to lower time direction and the bottom region of DE and JK will be widened. As the temperature is increased, D and J may ascend along *Y* axis, the intersection of PQ and CD will move to higher time direction, and the bottom region of DE and JK will be lessened. Correspondingly, DBT may occur at the time range of CD (or OJ).

4. Conclusions

The correlation of the crystalline structure development and corresponding tensile properties was studied for iPP and iPP/PEOc (80/20) blend by means of controlling isothermal crystallization to various levels, and the DBT was obtained and elucidated in terms of the crystallization conditions. Based on the present results, some concluding remarks can be drawn as follows.

The isothermal crystallization conditions including the crystallization temperature and time govern the crystalline morphology and eventually the tensile properties of iPP and the iPP/PEOc (80/20) blend. The lower the crystallization temperature, the shorter crystallization time is required for the appearance of DBT, and the sharper the transition will be. The addition of the elastomer phase will delay the occurrence of the transition for the iPP/PEOc blend. The crystallization temperature, crystallization time and the composition are all proven to be significant variables in determining the occurrence of the transition. These findings provide a new scope in controlling the DBT, and therefore they are of great significance in guiding the processing and treatment from industrial points of view.

Acknowledgement

The work was supported by National Natural Science Foundation of China (20490220 and 50773087). The author Y.Y. Pang thanked Prof. Z.G. Wang for helpful discussion.

References

[1] McNally T, McShane P, Nally GM, Murphy WR, Cook M, Miller A. Polymer 2002;43:3785–93.
[2] Da Silva ALN, Rocha MCG, Coutinho FMB, Bretas R, Scuracchio C. Polym Test 2000;19:363–71.
[3] Da Silva ALN, Rocha MCG, Coutinho FMB, Bretas R, Scuracchio C. J Appl Polym Sci 2000;75:692–704.
[4] Kontopoulou M, Wang W, Gopakumar TG, Cheung C. Polymer 2003;44:7495–504.
[5] Premphet K, Paecharoenchai W. J Appl Polym Sci 2002;85:2412–8.
[6] Yang JH, Zhang Y, Zhang YX. Polymer 2003;44:5047–52.
[7] Pang YY, Dong X, Zhao Y, Han CC, Wang DJ. Polymer 2007;48:6395–403.
[8] Du J, Niu H, Dong JY, Dong X, Wang DJ, He AH, et al. Macromolecules 2008;41:1421–9.
[9] Prieto Ó, Pereña JM, Benavente R, Cerrada ML, Pérez E. Macromol Chem Phys 2002;203:1844–51.
[10] Meng K, Dong X, Zhang XH, Zhang CG, Han CC. Macromol Rapid Commun 2006;27:1677–83.
[11] Pang YY, Dong X, Zhang XQ, Liu KP, Chen EQ, Han CC, et al. Polymer 2008;49:2568–77.
[12] Jiang W, Tjong SC, Li RKY. Polymer 2000;41:3479–82.
[13] Jiang W, Liu CH, Wang ZG, An LJ, Liang HJ, Jiang BZ, et al. Polymer 1998;39:3285–8.
[14] Borggreve RJM, Gaymans RJ, Schuijer J, Ingen Housz JF. Polymer 1987;28:1489–96.
[15] Jang BZ, Uhlmann DR, Vander Sande JB. J Appl Polym Sci 1984;29:3409–20.
[16] Matsushige K, Radcliffe SV, Baer E. J Appl Polym Sci 1976;20:1853–66.
[17] Samules RJ. Structured polymer properties: the identification, interpretation, and application of crystalline polymer structure. New York: John Wiley & Sons; 1974. p. 161–211.

[18] Kennedy MA, Peacock AJ, Mandelkern L. Macromolecules 1994;27:5297–310.
[19] Kennedy MA, Peacock AJ, Failla MD, Lucas JC, Mandelkern L. Macromolecules 1995;28:1407–21.
[20] Mandelkern L, Smith FL, Failla M, Kennedy MA, Peacock AJ. J Polym Sci Part B Polym Phys 1993;31:491–3.
[21] Wu SH. Polymer 1985;26:1855–63.
[22] Shan GF, Yang W, Yang MB, Xie BH, Feng JM, Fu Q. Polymer 2007;48:2958–68.
[23] Dlugosz J, Fraser GV, Grubb D, Keller A, Odell JA, Goggin PL. Polymer 1976;17:471–80.
[24] Hoffman JD, Weeks JJ. J Chem Phys 1965;42:4301–2.
[25] Wang ZG, Wang XH, Hsiao BS, Phillips RA, Medellin-Rodriguez FJ, Srinivas S, et al. J Polym Sci Part B Polym Phys 2001;39:2982–95.
[26] Shieh YT, Liu GL. J Polym Sci Part B Polym Phys 2007;45:466–74.
[27] Xu YX, Xu J, Guo BH, Xie XM. J Polym Sci Part B Polym Phys 2007;45:420–8.
[28] Yadav YS, Jain PC. Polymer 1986;27:721–7.
[29] Wang ZG, Phillips RA, Hsiao BS. J Polym Sci Part B Polym Phys 2000;38:2580–90.
[30] Robelin-Souffaché E, Rault J. Macromolecules 1989;22:3581–94.
[31] Ezquerra TA, Roslaniec Z, López-Cabarcos E, Baltà-Calleja FJ. Macromolecules 1995;28:4516–24.
[32] Bedia EL, Murakami S, Senoo K, Kohjiya S. Polymer 2002;43:749–55.